



Origin of broad molecular weight distribution of polyethylene produced by Phillips-type silica-supported chromium catalyst

Kiwamu Tonosaki, Toshiaki Taniike*, Minoru Terano

School of Materials Science, Japan Advanced Institute of Science and Technology, 1-1 Asahidai, Nomi, Ishikawa 923-1292, Japan

ARTICLE INFO

Article history:

Received 22 November 2010
Received in revised form 22 February 2011
Accepted 8 March 2011
Available online 15 March 2011

Keywords:

Phillips catalyst
Density functional theory
Molecular weight distribution
Polyethylene (PE)

ABSTRACT

The origin of the broad molecular weight distribution of polyethylene produced by Phillips-type silica-supported chromium (Cr/SiO_2) catalysts was studied by density functional calculations using active site models with various coordination environments. Difference of the coordination environment of chromium showed remarkable variations for both of the insertion and the chain transfer energies, resulting in a broad range of molecular weight from 10^2 to 10^{10} g/mol at 350 K. The results clarified that the special catalytic property of Cr/SiO_2 for broad molecular weight distribution is attributed to the heterogeneity of the coordination environment of the chromium species.

© 2011 Elsevier B.V. All rights reserved.

1. Introduction

Phillips catalysts [1] composed of CrO_x supported on SiO_2 (Cr/SiO_2) have long maintained their industrial importance after the discovery in 1950s in the polyolefin manufacture to produce nearly 7 million tons of a special grade of high density polyethylene (HDPE) per year over the world. The specialty of the Cr/SiO_2 catalysts is an ability to produce HDPE with fine mechanical properties such as elasticity and impact resistance, and with superior moldability due to its high melt viscosity. They come from both broad molecular weight distribution (MWD) and adequate amounts of short and long chain branches, which are automatically produced in ethylene homopolymerization [2]. As finer controls of polymer structures with the Cr/SiO_2 catalysts have been continuous demands for further multi-purpose materials, significant efforts still deposit obscurities in the mechanistic origin of the unique catalytic features.

The broad MWD has been believed to be mainly of a chemical origin, while some physical influences such as monomer concentration gradients within catalyst particles were also reported [3]. The chemical origin has been regarded as the heterogeneity of supported Cr species. Specifically, the conventional catalyst synthesized by an impregnation method makes a mixture of several types of potentially active Cr(VI) species and inactive Cr_2O_3 clusters [4–9]. In past years, many researchers have tried to investigate structures of Cr(VI) species. Applying UV–vis diffuse reflectance, Raman

and X-ray adsorption spectroscopies (XAS), Weckhuysen et al. [10] found mono- and dichromate with tetrahedral symmetry mainly present on the surface. Dichromate species are dominant among Cr(VI) at high Cr loadings and/or high calcination temperatures. However, since surface structures can be sensitive to the surface chemistry of oxide supports, the nuclearity of Cr(VI) is still under debate [11]. Furthermore, reduced Cr species, which are transient states between Cr(VI) and lower valence active species, exhibit a variation in the bonding and the interaction with surface oxygen. Such heterogeneity of coordination environment around Cr leads to a variety of symmetry and oxidation states of reduced Cr species. For example, UV–vis spectroscopy and XAS showed the presence of pseudo tetrahedral Cr(II), pseudo octahedral Cr(II) and pseudo octahedral Cr(III) on a reduced catalyst [12,13]. A recent report by Gianolio et al. [14] showed a direct evidence of the coordination of surface siloxane ligands to reduced Cr species by the EXAFS, which is believed to be crucial for giving a variety of coordination environments around reduced Cr species. In an IR study by Zecchina et al. [15–17], three types of reduced species were identified (named as species A, B and C) through the adsorption of CO. Thus, Cr species on SiO_2 can be roughly classified in terms of two kinds of heterogeneities: (1) nuclearity and (2) coordination environment.

Several Phillips-type model catalysts with uniform Cr structures have been designed in order to reduce the above-mentioned heterogeneity. For example, Amor Nait Ajjou and Scott [18–20] supported dialkylated Cr(IV) mononuclear species on SiO_2 by chemical vapor deposition (CVD) of CrNp_4 ($\text{Np} = \text{Neopentyl}$). Ikeda and Monoi reported a model catalyst with monoalkylated Cr(III) mononuclear species supported on SiO_2 , using a molecular precursor of $\text{Cr}(\text{CH}(\text{SiMe}_3)_2)_3$ [21]. Both of the model catalysts showed quite

* Corresponding author. Tel.: +81 761 51 1622; fax: +81 761 51 1625.
E-mail address: taniike@jaist.ac.jp (T. Taniike).

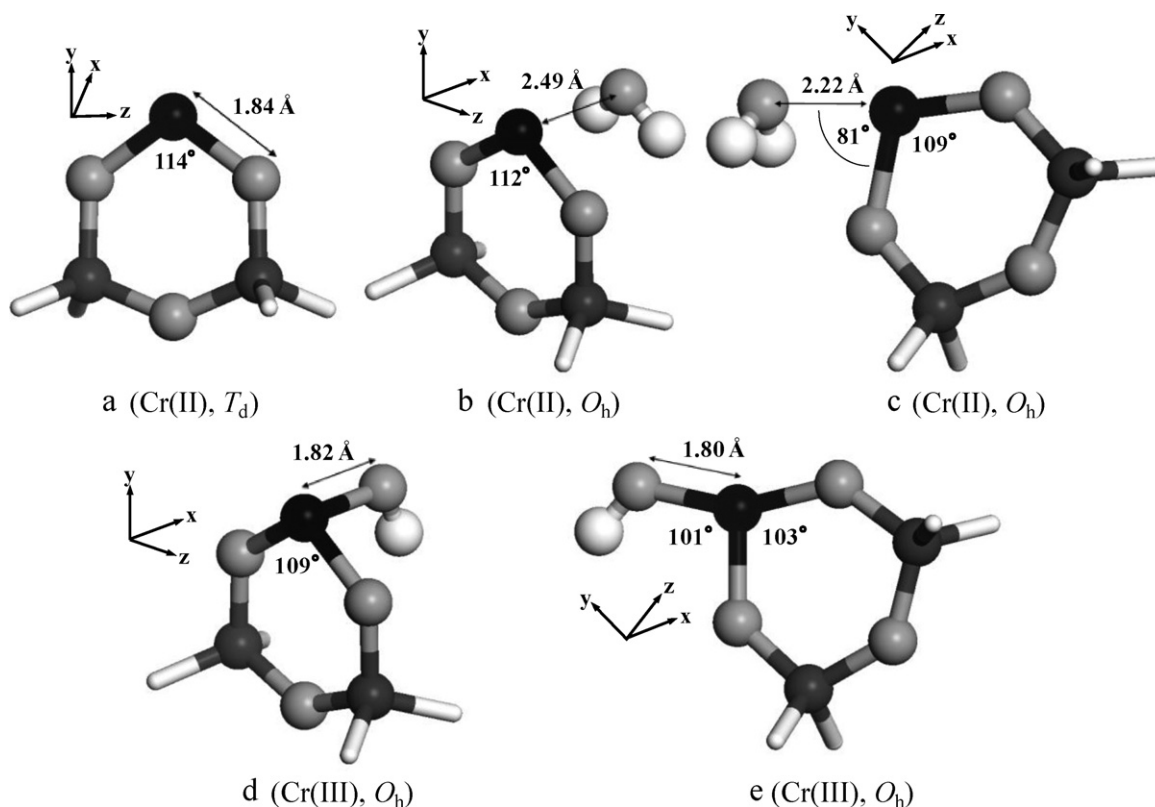


Fig. 1. Active site models with various coordination environments. Black: Cr, dark gray: Si, gray: O, white: H.

high activity for ethylene polymerization, and the MWDs of produced HDPEs were surprisingly very broad comparable with that obtained from impregnated catalysts, in spite of the almost uniform Cr nuclearity and oxidation state. It is believed that the heterogeneity of Cr species exists for these model catalysts due to the difference of the coordination environment around Cr species. On the other hand, Nenu et al. reported that an impregnated Cr/SiO₂ catalyst behaved like a single-site catalyst, giving very narrow MWD close to 2, when 1,3,5-tribenzylhexahydro-1,3,5-triazine was added as a coordinative ligand to Cr species [13,22,23]. Obviously, all these results suggest much larger contribution of the coordination environment of Cr to broaden MWD than that of the nuclearity.

In this contribution, we present the first molecular-level investigation for influences of coordination environments of Cr on the MW of PE. The apparent free energies of activation for the ethylene insertion to growing chain and chain transfer (CT) to coordinated ethylene were calculated by density functional theoretical (DFT) calculation for various active site models. The results obtained here have disclosed active site structures of Cr for broadening MWD of PE, and have provided valuable insights in the catalytic properties of Cr/SiO₂ catalysts as well as in molecular chemistry of these elemental reactions. To the best of our knowledge, DFT investigation on the origin of unique structures of produced PE by Phillips catalysts has never been undertaken so far.

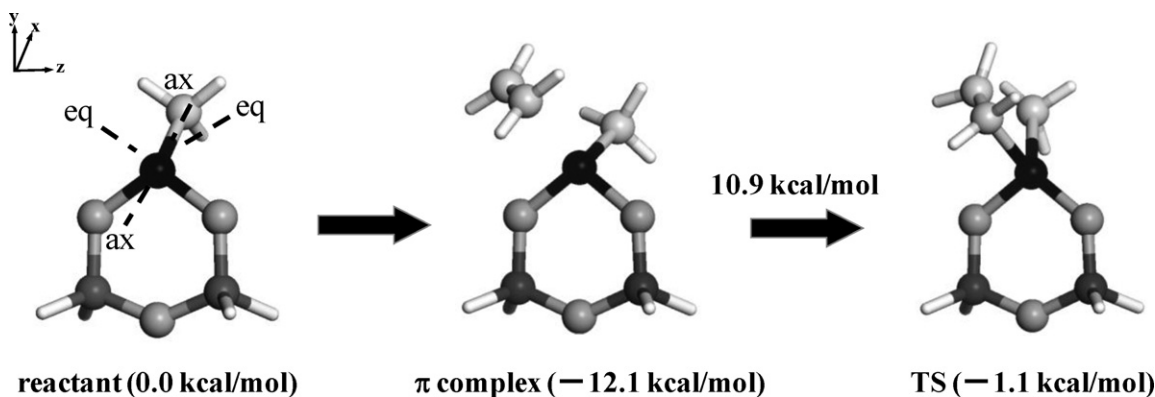
2. Numerical details

All the DFT results were obtained using DMol3 as implemented in the Materials Studio (Version 4.2) [24]. The exchange–correlation functional of Perdew–Burke–Ernzerhof [25] (PBE), which is one of the most frequently used functional on the study of catalytic reactions on heterogeneous metal oxide catalysts, was employed. The basis set was the double numeric with d-polarization functions

except for hydrogen (DND) combined with effective core potentials (ECP) [26,27]. The real space cutoff radius was 4.400 Å. The convergence criterion for SCF calculations was 1.0×10^{-5} Hartree, and those for geometry optimization were 2.0×10^{-5} Hartree for energy and 4.0×10^{-3} Hartree/Å for the maximum force. A high-spin state was always favored for Cr(IV), Cr(III) and Cr(II). Transition states (TS) of both ethylene insertion and CT reaction were obtained by TS optimization based on the Newton–Raphson algorithm. The CT reaction in ethylene polymerization with Cr/SiO₂ catalysts is known to mainly occur through β -hydrogen transfer to ethylene [28].

The size of the employed basis set was rather small in obtaining converged energies. Especially, the lack of diffuse functions on Cr leads to underestimation of the energies of π -complexes and TSs compared with the energy of gas-phase ethylene and a monomer-free active site, resulting in overestimation of π -complexation energies and underestimation of activation energies. However, as described later, the present task is to estimate the energetic difference between two activation energies (see Eq. (3)) rather than quantitative evaluation of the above values. Considering the cancellation of errors for differential values, the employed basis set could fulfill our target to compare MWs among various coordination environments. Actually the magnitude of MW estimated for the most basic active site (Fig. 1, model a) was the same when a larger basis set (DNP) and higher convergence criteria (fine) were employed.

To elucidate effects of coordination environments on the MW of PE, five cluster models a–e were employed in Fig. 1. Cr was basically supported on the minimum –O–Si(H₂)–O–Si(H₂)–O– framework, although the effects of the chromasiloxane ring size and those of the hydrogen termination were also investigated. Such 6-membered chromasiloxane ring was regarded as one of the most plausible species by Espelid and Børve [29], and Demmelmaier et al. reported



Scheme 1. Insertion pathway for (a). Black: Cr, dark gray: Si, gray: O, light gray: C, white: H.

that the 6-membered chromasiloxane was most easily activated by ethylene [30]. The model **a** possesses a tetrahedral symmetry, which have been employed in most of the previous calculations [29,31]. However, the presence of Cr(II) and Cr(III) situated in a distorted octahedral symmetry was also experimentally evidenced. Such octahedral species were modeled by adding a third ligand to the basic framework having two Cr–ester bonds. The third ligand is likely coordinative siloxane or silanol for Cr(II) and an additional Cr–ester bond for Cr(III) in real Cr/SiO₂ catalysts. We used coordinative H₂O and Cr–OH as these third ligands for Cr(II) and Cr(III), respectively. Electronic effects of H₂O and OH on Cr species were confirmed by us to be similar to those of (SiH₃)₂O and OSiH₃, respectively. Furthermore the H₂O and OH ligands enabled us to enforce a desired octahedral symmetry with the minimal steric effects, thus being suitable for our objective. Supposing that the chromasiloxane ring composes an equatorial plane with Cr at the origin, a series of octahedral Cr species was prepared by placing H₂O (**b** and **c**) or OH (**d** and **e**) at an axial or equatorial position.

The models **a–e** were firstly optimized without ethylene monomer as neutral Cr(II) or Cr(III) species, where the chromasiloxane ring was restricted in the YZ plane with the Cr atom fixed at the origin. The restriction of the chromasiloxane ring to the planar structure was essential to keep octahedral symmetry for **b–e**, and it hardly affected the results for **a**. In order to maintain the desired symmetries, the coordinating O atom of the H₂O ligand and all the atoms of the OH ligand allowed to relax along the axial direction on the X axis for the models **b** and **d**, or within the equatorial face on the YZ plane for the models **c** and **e**. Thus obtained Cr(II) and Cr(III) atoms with different coordination environments were employed in subsequent calculations for ethylene polymerization, where the position of the H₂O and OH ligands was fixed in order to keep the desired symmetry. The fixation of the third ligands might more or less overestimate their influences on the polymerization properties, but we believed that the obtained results qualitatively are held for the real surface, where the position of third ligands must be constrained.

The most probable MW (*MW*) of PE under the dominance of the CT to ethylene is given by

$$\frac{MW}{28.06} = \bar{P}_n = \frac{k_p}{k_{tr}} \quad (1)$$

where \bar{P}_n , k_p and k_{tr} are the most probable polymerization degree, and the rate constants for the propagation (insertion) and of the CT, respectively. Making use of

$$k_{p/tr} = \frac{RT}{N_A h} \exp\left(\frac{-\Delta G_{p/tr}^\ddagger}{RT}\right) \quad (2)$$

Eq. (1) becomes

$$\frac{MW}{28.06} = \exp\left(\frac{-\Delta G_p^\ddagger - \Delta G_{tr}^\ddagger}{RT}\right) \quad (3)$$

where R , N_A , ΔG_p^\ddagger and ΔG_{tr}^\ddagger are the gas constant, the Avogadro constant and the apparent Gibbs energies of activation for the propagation and the CT, respectively.

3. Results and discussion

Effects of the coordination environments on *MW* were mainly investigated for monoalkyl-Cr(III) and -Cr(IV) (alkyl: methyl or *n*-propyl) active species. Although some recent experimental results suggested the possibility of dialkyl-Cr(IV) active species for the propagation [18–20,32], we found that a π -complex was not formed at both dimethyl-Cr(IV) and chromacyclopentane(IV) species, and the activation energies for the ethylene insertion into the dimethyl-Cr(IV) and chromacyclopentane(IV) were 13.0 and 24.8 kcal/mol, respectively, higher than that into monomethyl-Cr(III). The difficulty of ethylene insertion to the dialkyl-Cr(IV) and chromacycloalkane(IV) has been also reported by Espelid and Børve [29].

An ethylene insertion pathways on monomethyl-Cr(III) of **a** is described in Scheme 1. Even if the model **a** was situated in tetrahedral symmetry, the ethylene insertion proceeded at octahedral sites. The methyl group was oriented to an axial position and the ethylene coordinated at an equatorial position. The structure of the π -complex with the methyl group at an equatorial position and coordinated ethylene at an axial position was 20.0 kcal/mol less stable than the most stable one. Thus, the alkyl and the hydride disfavored the trans position of O ligands, especially for covalently bonding O. On the contrary, π coordination preferred the trans position of O ligands. Those trans influences caused significant differences in ethylene polymerization properties of monoalkyl-Cr species with additional H₂O and OH ligands, which is described below.

Table 2 shows the energies of the ethylene coordination, insertion and β -hydrogen transfer to ethylene for Cr-*n*-propyl situated in various coordination environments together with the most probable MWs of PE produced at each active site. Exceptionally, **d** could not accept π -complexation since *n*-propyl was strongly forced to a tetrahedral position to escape from the trans position of the three covalent O. The existence of the third ligands reduced the adsorption energies of the ethylene (ΔE_{ad}) regardless those electronic properties and positions, suggesting that the third ligands sterically narrowed the coordination space for ethylene. The apparent activation energies (ΔE_{ap}) of the ethylene insertion into Cr-*n*-propyl were basically increased by the presence of the third ligand

Table 1
Effects of coordination environment for activation energies and MW of produced PE^a.

Model	ΔE_{ad}^b	ΔE_{ap}^c		$\Delta G_p^\ddagger - \Delta G_{tr}^\ddagger$	MW
		Insertion	CT		
a	-12.0	-1.1	7.0	-4.8	2.8×10^4
b	-8.2	4.3	24.2	-15.0	7.0×10^{10}
c	-8.2	0.4	6.2	-2.4	8.6×10^2
d	-	21.3	-	-	-
e	-7.7	4.9	6.7	0.7	~ 0

^a Energies are in kcal/mol.

^b ΔE_{ad} is the adsorption energy of ethylene.

^c ΔE_{ap} is the apparent activation energy, the height of the TS before π complexation.

^d ΔG_p^\ddagger and ΔG_{tr}^\ddagger are the Gibbs energies of activation for the insertion and CT at 350 K.

compared with the value for **a**, and the degree of the increase was dependent on the position and kind of the ligands. For the β -hydrogen transfer to coordinated ethylene, the ligands at an equatorial position hardly affected ΔE_{ap} for **c** and **e** compared with that for **a**. On the contrary, ΔE_{ap} became much higher for **b** and **d**, with the ligands at an axial position, than that for **a**. Especially, even a TS was not obtained for **d**.

ΔG^\ddagger was calculated for both the insertion and CT in order to incorporate the influences of the temperature into account. The temperature was set to 350 K, typical for industrial ethylene polymerization with Cr/SiO₂ catalysts. Table 1 shows $\Delta G_p^\ddagger - \Delta G_{tr}^\ddagger$, whose exponential gives the most probable MW based on Eq. (3). The values of $\Delta G_p^\ddagger - \Delta G_{tr}^\ddagger$ are only 1.0–4.6 kcal/mol higher than those of $\Delta E_p^\ddagger - \Delta E_{tr}^\ddagger$, which means that the entropic contribution slightly enhances CT compared with the insertion. On the other hand, the variation of the $\Delta G_p^\ddagger - \Delta G_{tr}^\ddagger$ values among the different active site models is similar to that of the $\Delta E_p^\ddagger - \Delta E_{tr}^\ddagger$ values, indicating that the variation of MWs is mostly decided by the electronic contribution.

For monoalkyl-Cr(III) in different coordination environments **a–c**, the variation of the energetic difference between the insertion and CT enabled a wide range of MWs from 8.6×10^2 to 7.0×10^{10} . The coordination of H₂O at the axial position led to a higher MW as a result of the inhibited CT, and that at the equatorial position to a lower MW. As for monoalkyl-Cr(IV), the enchainment did not proceed for **e** at 350 K in consequence of the relative enhancement of the CT. The π -complex was not formed for **d**. Thus, monoalkyl-Cr(IV) species were not likely relevant in the ethylene polymerization with Cr/SiO₂ catalysts.

Though the results presented here assumed rather ideal tetrahedral or octahedral symmetry, probably leading to quantitative over- or under-estimation, it could be safely concluded that one of the dominant factors of the broad MWD of PE produced by Cr/SiO₂ catalysts is the coordination environment of Cr. Also, the O–Cr–O

Table 2
Effects of chromasiloxane ring size for activation energies and MW of produced PE^a.

Ring	ΔE_{ad}^b	ΔE_{ap}^c		$\Delta G_p^\ddagger - \Delta G_{tr}^\ddagger$	MW
		Insertion	CT		
4-Membered	-15.4	-4.4	1.6	-3.2	2.7×10^3
6-Membered	-12.0	-1.1	7.0	-4.8	2.8×10^4
8-Membered	-8.2	0.8	8.8	-6.6	3.9×10^5

^a Energies are in kcal/mol.

^b ΔE_{ad} is the adsorption energy of ethylene.

^c ΔE_{ap} is the apparent activation energy, the height of the TS from the reactant before π complexation.

^d ΔG_p^\ddagger and ΔG_{tr}^\ddagger are the Gibbs energies of activation for the propagation and CT at 350 K.

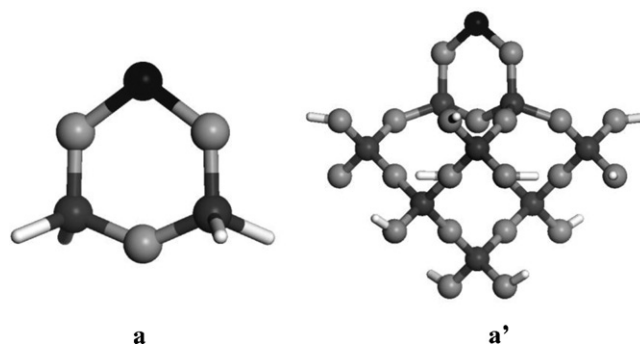


Fig. 2. Cluster models with a 6-membered chromasiloxane structure. Black: Cr, dark gray: Si, gray: O, white: H.

angle of a chromasiloxane ring has been considered as one of the decisive factors for the polymerization activity [30]. However in our calculations (Table 2), it was much less associated with MWD of produced PE, while the activity was surely influenced by it.

To confirm the effects of the hydrogen termination, a larger cluster model named as **a'** was employed with a 6-membered chromasiloxane structure (Fig. 2). **a'** was cut off from a (100) surface of β -crystalalite. Surfaces of amorphous SiO₂ has been explained as a mixture of the (100) and (111) surfaces of β -crystalalite [33], and the dehydroxylated (100) surface was reported to stabilize a 6-membered metallasiloxane [34,35]. The edge parts of the cluster were again capped with hydrogen in order to keep electronic neutrality. All atoms in the SiO₂ support except those in the chromasiloxane framework were fixed during calculations. As shown in Table 3, the larger cluster **a'** increased the π -complexation energy compared with that of the minimal cluster **a**, resulting in similar reductions of the ΔE_{ap} values for insertion and CT. Consequently, the resulting MW of produced PE was almost similar with that of **a**. Thus, the effects of the cluster size for the support on MW could be regarded to be much less important than those of the coordination environment.

To address the origin of the effects of the coordination environment on the insertion and CT, the elemental activation barriers, ΔE_{el} , was decomposed according to

$$\Delta E_{ap} = \Delta E_{ad} + \Delta E_{el} = \Delta E_{ad} + \Delta E_{detach} + \Delta E_{M-C} + \Delta E_{def} + \Delta E_{M-TS} + \Delta E_{attach} \quad (4)$$

The energetic decomposition was conducted based on Scheme 2, where ethylene and alkyl anion were stepwisely separated from a chromasiloxane cation for both a π -complex and TS, and the energies of the separated fragments were calculated without geometry optimization. A similar decomposition was previously reported by Margl et al. [36,37]. ΔE_{detach} and ΔE_{attach} indicate the binding force of ethylene. ΔE_{M-C} and ΔE_{M-TS} indicate the Cr-alkyl bond strength

Table 3
Effects of the cluster size on the activation energies and MW of produced PE^a.

Model	ΔE_{ad}^b	ΔE_{ap}^c		$\Delta G_p^\ddagger - \Delta G_{tr}^\ddagger$	MW
		Insertion	CT		
a	-12.0	-1.1	7.0	-4.8	2.8×10^4
a'	-12.5	-1.7	5.8	-4.7	2.4×10^4

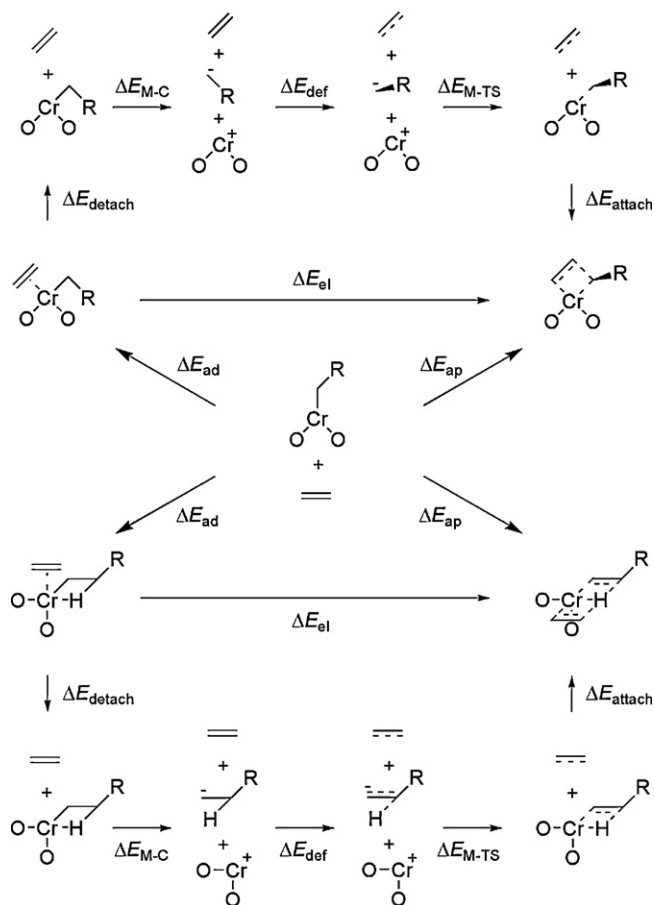
^a Energies are in kcal/mol.

^b ΔE_{ad} is the adsorption energy of ethylene.

^c ΔE_{ap} is the apparent activation energy, the height of the TS from the reactant before π complexation.

^d ΔG_p^\ddagger and ΔG_{tr}^\ddagger are the Gibbs energies of activation for the propagation and CT at 350 K.

Insertion



Chain Transfer

Scheme 2. Schematic representation of decomposition of the activation barriers.

for a π -complex and TS, respectively. ΔE_{def} is the deformation energy of the fragments in the transformation from a π -complex to TS. All the values shown in Table 4 are differential values from those for **a**. As explained in the discussions for Table 2, the existence of the third ligand sterically prevented the ethylene coordination to increase ΔE_{ad} . Correspondingly, ΔE_{detach} decreased in the presence of the third ligand. However, the sum of $\Delta \Delta E_{\text{ad}}$ and $\Delta \Delta E_{\text{detach}}$ are not necessarily zero, since the sum contains the degree of the deformation in forming a π -complex. As for **b**, the sum of $\Delta \Delta E_{\text{ad}}$ and $\Delta \Delta E_{\text{detach}}$ is almost zero, indicating that the third ligand at the axial position induced a similar degree of structural distortion of the π -complex to that for **a**. The distortion is larger for **c** with the

positive value, and smaller for **e** with the minus value for the sum of $\Delta \Delta E_{\text{ad}}$ and $\Delta \Delta E_{\text{detach}}$ for the insertion. The third ligand at the equatorial position altered the degree of the distortion in forming the π -complexes, and the direction of the alternation was opposite for electron donating H_2O and accepting OH. In the case of CT, the ethylene coordination took place at the axial position of Cr for **c** and **e**, since the equatorial position was occupied with β -hydrogen of alkyl. Much weaker coordination of ethylene to the axial position significantly reduces the distortion in forming the π -complexes, where the absolute values of ΔE_{ad} and ΔE_{detach} are almost equal. As shown in $\Delta \Delta E_{\text{M-C}}$ for both insertion and CT, the Cr-*n*-propyl bond tended to be destabilized (decrease of $\Delta \Delta E_{\text{M-C}}$) by H_2O and ethylene, both electron donors, especially when they coordinated to the equatorial position. This was due to effective electron donation from the ligands at the equatorial position to the Cr-ester bond. On the contrary, OH, an electron acceptor, at the equatorial position slightly stabilized the Cr-*n*-propyl bond (increase of $\Delta \Delta E_{\text{M-C}}$). ΔE_{def} for the insertion is higher for **b**, having a more deformed TS, than for **a**. For **b**, an axial position, which would have stabilized the newly forming alkyl, was already filled by H_2O . Meanwhile, when the third ligands came to the equatorial position for **c** and **e**, the symmetry of the active site was forced to be bipyramidal, and then the distortion in TS for the insertion became slightly smaller than that for **a**. In CT, a significant increase of ΔE_{def} is observed for **b**, since both the newly forming ethyl and hydride were enforced to the unfavorable equatorial position by H_2O at TS. The influences of ligands on $\Delta \Delta E_{\text{M-TS}}$ and $\Delta \Delta E_{\text{attach}}$ for both the insertion and CT are similar to those on $\Delta \Delta E_{\text{detach}}$ and $\Delta \Delta E_{\text{M-C}}$, even though the location of each TS affects $\Delta \Delta E_{\text{detach}}$ and $\Delta \Delta E_{\text{M-C}}$.

Table 5 summarizes the energetic effects of the additional ligand for the key steps in the ethylene insertion and CT. $\Delta E_{\pi-R}$ in Table 5 is the difference of the binding forces of ethylene and alkyl to Cr between a π -complex and TS, defined as,

$$\Delta E_{\pi-R} = (\Delta E_{\text{detach}} + \Delta E_{\text{M-C}}) - (\Delta E_{\text{M-TS}} + \Delta E_{\text{attach}}) \quad (5)$$

In the cases of the ethylene insertion, $\Delta E_{\pi-R}$ shows insignificant differences among the three monoalkyl-Cr(III), **a**, **b**, and **c**. As a result, the most important contribution of the additional ligand, H_2O , was on the increase of ΔE_{ad} , which led to elevate ΔE_{ap} compared with that of **a**. Then, the final values of ΔE_{ap} were modulated by ΔE_{def} according to the position of H_2O . Espelid and Børve reported that Cr(IV) was less active for the ethylene insertion due to the weak coordination of ethylene [29]. This is also seen in ΔE_{ad} for **e**. In addition, a higher $\Delta E_{\pi-R}$ indicating the destabilized Cr-fragment bondings at TS also increased ΔE_{ap} . The oxidation state of monoalkyl-Cr is not important for CT as seen in ΔE_{ap} of **c** and **e**, where $\Delta \Delta E_{\text{def}}$ is nearly zero, and $\Delta \Delta E_{\pi-R}$ and $\Delta \Delta E_{\text{ad}}$ are well canceled to have a similar ΔE_{ap} to that of **a**. The highest ΔE_{ap} for **b** obviously arises from high ΔE_{def} indicating the decisive contribution of the structural distortion of TS for CT.

Table 4
Decomposition of the activation barriers for the ethylene insertion and CT^a.

Reaction	Model	$\Delta \Delta E_{\text{ad}}$	$\Delta \Delta E_{\text{detach}}$	$\Delta \Delta E_{\text{M-C}}$	$\Delta \Delta E_{\text{def}}$	$\Delta \Delta E_{\text{M-TS}}$	$\Delta \Delta E_{\text{attach}}$	$\Delta \Delta E_{\text{ap}}$
Insertion	a	0.0 (−12.0)	0.0 (16.0)	0.0 (254.5)	0.0 (14.1)	0.0 (−240.8)	0.0 (−32.9)	0.0 (−1.1)
	b	3.8	−4.1	−8.2	0.2	12.2	1.5	5.4
	c	3.8	−1.2	−20.0	−0.8	21.9	−2.2	1.5
	e	4.3	−7.3	1.6	−3.4	4.0	6.8	6.0
CT	a	0.0 (−12.0)	0.0 (16.0)	0.0 (254.5)	0.0 (24.5)	0.0 (−259.4)	0.0 (−16.5)	0.0 (7.0)
	b	3.8	−4.1	−8.2	17.0	15.6	−6.8	17.2
	c	6.8	−10.4	−11.2	−0.7	19.4	−4.8	−0.6
	e	7.1	−10.9	5.7	−2.2	1.8	−1.8	−0.3

^a Energies are in kcal/mol. All $\Delta \Delta E$ components whose definition is illustrated in Scheme 2 are differential values from ΔE for **a** written in the parentheses.

Table 5
Simplified decomposition of the activation barriers for the ethylene insertion and CT^a.

Reaction	Model	$\Delta\Delta E_{ad}^a$	$\Delta\Delta E_{\pi-R}^b$	$\Delta\Delta E_{def}^a$	$\Delta\Delta E_{ap}^a$
Insertion	a	0.0 (–12.0)	0.0 (–2.3)	0.0 (14.1)	0.0 (–1.1)
	b	3.8	1.4	0.2	5.4
	c	3.8	–1.5	–0.8	1.5
	e	4.3	5.1	–3.4	6.0
CT	a	0.0 (–12.0)	0.0 (–5.4)	0.0 (24.5)	0.0 (7.0)
	b	3.8	–3.5	17.0	17.2
	c	6.8	–7.0	–0.7	–0.6
	e	7.1	–5.2	–2.2	–0.3

^a Energies are in kcal/mol.^b $\Delta\Delta E_{\pi-R}$ shows the difference of the binding strength of ethylene and alkyl fragments to Cr between at TS and at π complex, which is defined as Eq. (5).

4. Conclusions

The heterogeneity of the interaction of Cr with SiO₂ supports generates a variety of Cr species situated in different coordination environments in industrial Cr/SiO₂ ethylene polymerization catalysts. In this density functional study, we have investigated the effects of the coordination environment around Cr active species on the molecular weight of produced polyethylene. On the basis of chromasiloxane having two Cr–O–Si bonds, various kinds of alkyl–Cr species were modeled by adding suitable third ligands such as H₂O and OH to an equatorial or axial position of the basic chromasiloxane structure. H₂O and OH mimicked a coordinative O of siloxane or silanol and an additional O covalently bound to Cr, respectively. The results obtained are summarized briefly as follows. The molecular weight of produced polyethylene at monoalkyl–Cr(III) species was significantly sensitive to the additional ligand. The coordinative O at the equatorial position increased the activation energy of ethylene insertion through the reduction of the π -complexation energy, leading to a lower molecular weight ($\sim 10^2$). On the contrary, the O at the axial position led to a higher molecular weight ($\sim 10^{10}$), since the chain transfer was significantly inhibited in a steric reason. The basic bipodal monoalkyl–Cr(III) species gave intermediate molecular weights ($\sim 10^{3-5}$), depending on the size of the chromasiloxane ring. Monoalkyl–Cr(IV) species were not active for the ethylene polymerization. Thus, the characteristic broad molecular weight distribution of polyethylene produced by Phillips catalysts is concluded to be originated from the heterogeneity of coordination environments for monoalkyl–Cr(III) species on SiO₂. This study suggests a possibility for finer control of a molecular weight and its distribution in polyethylene production with Cr-based supported oxide catalysts. Modification of the distribution of surface hydroxyl groups or surface chemical treatment which introduces different Lewis basic sites is a plausible way to control the coordination environment of active species.

References

- [1] J.P. Hogan, R.L. Banks, U.S. Patent 2,825,721, 1958.
- [2] M.P. McDaniel, Adv. Catal. 33 (1985) 47.
- [3] M.P. McDaniel, J. Catal. 261 (2009) 34.
- [4] B. Liu, M. Terano, J. Mol. Catal. A: Chem. 172 (2001) 227.
- [5] B. Liu, Y. Fang, M. Terano, J. Mol. Catal. A: Chem. 219 (2004) 165.
- [6] Y. Fang, B. Liu, M. Terano, J. Mol. Catal. A: Chem. 131 (2005) 279.
- [7] M.P. McDaniel, J. Catal. 67 (1981) 71.
- [8] M.P. McDaniel, J. Catal. 76 (1982) 17.
- [9] M.P. McDaniel, J. Catal. 76 (1982) 29.
- [10] B.M. Weckhuysen, L.M. De Ridder, R.A. Schoonheydt, J. Phys. Chem. 97 (1993) 4756.
- [11] J.M. Jehng, I.E. Wachs, B.M. Weckhuysen, R.A. Schoonheydt, J. Chem. Soc. Faraday Trans. 97 (1993) 4756.
- [12] B.M. Weckhuysen, I.E. Wachs, R.A. Schoonheydt, Chem. Rev. 96 (1996) 3327.
- [13] C.N. Nenu, J.N.J. van Lingen, F.M.F. de Groot, D.C. Koningsberger, B.M. Weckhuysen, Chem. Eur. J. 12 (2006) 4756.
- [14] D. Gianolio, E. Groppo, J.G. Vitillo, A. Damin, S. Bordiga, A. Zecchina, C. Lamberti, Chem. Commun. 46 (2010) 976.
- [15] G. Ghiotti, E. Garrone, A. Zecchina, J. Mol. Catal. A: Chem. 46 (1988) 61.
- [16] G. Ghiotti, E. Garrone, A. Zecchina, J. Mol. Catal. A: Chem. 65 (1991) 73.
- [17] A. Zecchina, G. Spoto, G. Ghiotti, E. Garrone, J. Mol. Catal. A: Chem. 86 (1994) 423.
- [18] J. Amor Nait Ajjou, S.L. Scott, V. Paquet, J. Am. Chem. Soc. 120 (1998) 415.
- [19] J. Amor Nait Ajjou, S.L. Scott, J. Am. Chem. Soc. 122 (2000) 8968.
- [20] S.L. Scott, J. Amor Nait Ajjou, Chem. Eng. Sci. 56 (2001) 4155.
- [21] H. Ikeda, T. Monoi, J. Polym. Sci. A: Polym. Chem. 41 (2002) 413.
- [22] C.N. Nenu, B.M. Weckhuysen, Chem. Commun. (2005) 1865.
- [23] C.N. Nenu, B. Philippe, B.M. Weckhuysen, J. Mol. Catal. A: Chem. 269 (2007) 5.
- [24] B. Delley, J. Phys. Chem. 92 (1990) 508.
- [25] J.P. Perdew, K. Burke, M. Ernzerhof, Phys. Rev. Lett. 77 (1996) 3865.
- [26] M. Dolg, U. Wedig, H. Stoll, H. Preuss, J. Chem. Phys. 86 (1987) 866.
- [27] A. Bergner, M. Dolg, W. Kuechle, H. Stoll, H. Preuss, Mol. Phys. 80 (1993) 1431.
- [28] R. Blom, A. Follestad, O. Noel, J. Mol. Catal. 91 (1994) 237.
- [29] Ø. Espelid, K.J. Børve, J. Catal. 195 (2000) 125.
- [30] C.A. Demmelmaier, R.E. White, J.A. van Bokhoven, S.L. Scott, J. Catal. 262 (2008) 44.
- [31] Ø. Espelid, K.J. Børve, J. Catal. 205 (2002) 366.
- [32] E. Groppo, C. Lamberti, S. Bordiga, G. Spoto, A. Zecchina, J. Catal. 240 (2006) 172.
- [33] I.S. Chuang, G.E. Maciel, J. Phys. Chem. B 101 (1997) 3052.
- [34] J.J. Mortensen, M. Parrinello, J. Phys. Chem. B 104 (2000) 2901.
- [35] J. Handzlik, J. Phys. Chem. C 111 (2007) 9337.
- [36] P. Margl, L. Deng, T. Ziegler, J. Am. Chem. Soc. 120 (1998) 5517.
- [37] P. Margl, L. Deng, T. Ziegler, J. Am. Chem. Soc. 121 (1999) 154.